



HAL
open science

Hydrous RuO₂ /carbon nanowalls hierarchical structures for all-solid-state ultrahigh-energy-density micro-supercapacitors

Ty Mai Dinh, Amine Achour, Sorin Vizireanu, Gheorghe Dinescu, Leona Nistor, Kevin Armstrong, Daniel Guay, David Pech

► To cite this version:

Ty Mai Dinh, Amine Achour, Sorin Vizireanu, Gheorghe Dinescu, Leona Nistor, et al.. Hydrous RuO₂ /carbon nanowalls hierarchical structures for all-solid-state ultrahigh-energy-density micro-supercapacitors. *Nano Energy*, 2014, 10, pp.288 - 294. 10.1016/j.nanoen.2014.10.003 . hal-01873388

HAL Id: hal-01873388

<https://laas.hal.science/hal-01873388>

Submitted on 13 Sep 2018

HAL is a multi-disciplinary open access archive for the deposit and dissemination of scientific research documents, whether they are published or not. The documents may come from teaching and research institutions in France or abroad, or from public or private research centers.

L'archive ouverte pluridisciplinaire **HAL**, est destinée au dépôt et à la diffusion de documents scientifiques de niveau recherche, publiés ou non, émanant des établissements d'enseignement et de recherche français ou étrangers, des laboratoires publics ou privés.

Hydrous RuO₂/carbon nanowalls hierarchical structures for all-solid-state ultrahigh-energy-density micro-supercapacitors

Ty Mai Dinh^{a,b,1}, Amine Achour^{a,b,1}, Sorin Vizireanu^c, Gheorghe Dinescu^c, Leona Nistor^d, Kevin Armstrong^e, Daniel Guay^e, and David Pech^{a,b,*}

^aCNRS, LAAS, 7 avenue du colonel Roche, F-31400 Toulouse, France.

^bUniv de Toulouse, LAAS, F-31400 Toulouse, France.

^cNational Institute for Laser, Plasma and Radiation Physics, Magurele, Bucharest, 077125 Romania.

^dNational Institute for Materials Physics, Magurele, Bucharest, 077125 Romania.

^eINRS-Énergie, Matériaux, Télécommunications, 1650 boulevard Lionel Boulet, J3X 1S2 Varennes, Québec, Canada.

*Corresponding author. Tel.: +33 5 61 33 68 37. *E-mail adress* : dpech@laas.fr (D. Pech).

¹These authors contributed equally to this work.

Abstract

Micro-supercapacitors have attracted considerable research attention for on-chip energy storage due to their unique properties and potential applications in various smart electronic devices. Although significant advances have been reported on their power performances, they still cannot compete with micro-batteries in terms of energy densities for mobile, portable and self-powered applications. Herein, we demonstrate the fabrication of vertically aligned carbon nanowalls (CNW) decorated with porous ruthenium oxide as a high-performance electrode for all-solid-state micro-supercapacitors. The decorated CNW electrode, essentially consisting of thin carbon sheets assembled from graphene domains, delivers specific capacitance in excess of 1000 mF cm^{-2} (which is three orders of magnitude higher than state-of-the-art micro-supercapacitors) and energy density comparable to that of lithium-ion micro-batteries, but with superior power and cycling stability. Our findings demonstrate a route towards the integration of microfabricated supercapacitors combining fast charge/discharge rates with high energy densities.

KEYWORDS: Micro-supercapacitor; Carbon nanowalls; RuO₂; Gel electrolyte

Introduction

The increasing importance of portable and wearable devices incorporating more advanced electronic technologies, as well as the future deployment of wireless sensor networks embedded in our everyday environment has made on-board energy storage a critical issue [1]. In the last decade, the integration of miniaturised electrochemical capacitors (also called supercapacitors) on circuit chips has been the subject of intense research on the account of their excellent charge-discharge rate and long operating life time [2-7]. Although ultrahigh-power micro-sized supercapacitors have been reported [8-14], they still suffer from low energy density that remains far from Li-ion micro-batteries [15-17]. A significant improvement of their volumetric/areal energy density is needed for more challenging applications.

Supercapacitors can be divided into two categories, depending on their charge-storage mechanism. The most common devices rely on the capacitive behaviour of high surface area carbon-based materials. The second category relies on the fast and reversible faradaic surface reactions of pseudo-capacitive materials, mainly transition metal oxides. Hydrated forms of ruthenium dioxide (hRuO_2) currently represent the state of the art among pseudo-capacitive materials, with the highest reported specific capacitance [18]. Its high cost has limited its development for large-size supercapacitors, but the use of this material becomes relevant and promising for micro-supercapacitors as very little amount of active material is required. Moreover, the capacitance of hRuO_2 can be further increased by deposition onto a nanostructured conductive support with high surface area such as carbon nanotubes [19], graphene [20,21] or porous gold [22].

Carbon nanowalls (CNW), also named vertically oriented graphene sheets, are among the most promising materials in the carbon family. They can be described as three-dimensional

networks of vertically standing, interconnected 2-D nanostructures consisting of graphene domains overlapping each other. This graphene-based architecture with vertical wall orientation, sharp edges and open structure is associated with a large surface area (in the range of 100-1500 m² g⁻¹) [23], good electronic conductivity [24] and excellent chemical stability [25]. These combined properties make carbon nanowalls superior for various electrochemical applications. Indeed, this nanostructured material has already been adopted in the semiconductor technology, but there have been very few reports for energy storage applications [26,27].

Herein, we demonstrate a new hybrid material based on capacitive CNW decorated with pseudo-capacitive hRuO₂. By adjusting the experimental synthesis conditions of the CNW and the electrodeposition parameters of hRuO₂, we achieved an outstanding specific capacitance of 1097 mF cm⁻², which is three orders of magnitude higher than state-of-the-art graphene based micro-supercapacitors [11]. Therefore, hRuO₂-decorated CNW electrode could be used to fabricate miniaturized energy-storage devices that bridge the massive energy density gap between supercapacitors and batteries, while still retaining extended lifetime and huge power density.

Materials and methods

Fabrication of the composite electrode

An insulating Si₃N₄ layer (80 nm) was first deposited on a silicon wafer. Current collectors were then deposited using the evaporation of a 40 nm Cr/200 nm Pt layer. The CNW layers growth was carried out by PECVD in a Ar/H₂/C₂H₂ radiofrequency plasma jet [28]. The plasma source operated at 400 W power, and 1400 sccm gas flow rate was used to produce, via a nozzle, a directional argon jet in the deposition chamber. Acetylene (1 sccm) and hydrogen (25 sccm)

were injected into this jet through a ring placed downstream the nozzle. The deposition proceeded on the heated substrate (700 °C) placed at 5 cm from the injection ring at a pressure of 1.3 mbar.

Electrodeposition of hydrous ruthenium oxide onto the CNW support was afterwards carried out from an aqueous chloride solution composed of 10 mM $\text{RuCl}_3 \cdot x\text{H}_2\text{O}$ in 10^{-1} M KCl / 10^{-2} M HCl, and adjusted to pH=2.5 with a 2M KOH aqueous solution. Cyclic voltammetry (CV) between -300 and +950 mV vs. saturated Ag/AgCl at 50 mV s^{-1} and performed at 50°C for various number of cycles under stirring conditions was used to induce the growth of the hRuO_2 deposits. All samples were annealed under air at 150°C for 1 h.

The PVA- H_3PO_4 -SiWA polymer precursor solution was prepared by mixing a poly(vinyl alcohol) (PVA, $M_w = 31\,000\text{-}50\,000$, 87-89 % hydrolyzed) solution with phosphoric acid (H_3PO_4) and SiWA ($\text{H}_4\text{SiW}_{12}\text{O}_{40}$) in a composition of 1.7 wt.% PVA, 1.9 wt.% H_3PO_4 , 14.4 wt.% SiWA and 82 wt.% de-ionized water. The conductivity of the solid electrolyte was 6.1 mS cm^{-1} after 24 h (22.2°C - 32 % RH).

Material characterization

Scanning electron microscopy (SEM) was performed using a Hitachi S-4800 field-emission electron microscope, and high resolution transmission electron microscopy (HRTEM) using an atomic resolution analytical Jeol JEM-ARM 200F electron microscope operating at 200 kV. Specimens for TEM observations were prepared by extracting CNW/ RuO_2 film flakes and transferring them on holey carbon grids. The Raman spectrum was recorded at 532 nm laser excitation wavelength, using a Jasco NRS 7200 apparatus. The surface chemical composition of

ruthenium oxide was estimated *via* X-ray Photoelectron Spectroscopy (XPS) using a Thermo Scientific spectrometer operating with a monochromatic AlK_{α} X-ray source (1486.6 eV).

Electrochemical characterization

The electrochemical characterizations were performed with a SP-240 potentiostat from BioLogic. A three-electrode electrochemical cell with a platinum gauze counter-electrode and a saturated Ag/AgCl reference-electrode in de-aerated 0.5 M H_2SO_4 electrolyte at room temperature was used for the electrode characterization (exposed area 1 cm^2), and a two-electrode cell with a PVA- H_3PO_4 -SiWA solid electrolyte for the device. Electrochemical Impedance Spectroscopy measurements were carried out at open circuit potential in the 100 kHz to 10 mHz frequency range. The accessibility of the electrolyte to the electroactive material has been investigated by calculating the voltammetric charge (q^*) as a function of the sweep rates (ν) according to a procedure developed by Trasatti [29,30]. The value of the outer capacitance (C_o) has been obtained from the extrapolation of q^* to $\nu = \infty$ from the plot of q^* vs. $\nu^{-1/2}$, whereas the total capacitance (C_t) has been estimated from the extrapolation of q^* to $\nu = 0$ from the plot q^{*-1} vs. $\nu^{1/2}$.

Results and discussion

Figure 1a shows the top-view scanning electron microscope (SEM) image of a CNW layer deposited on a silicon wafer (which was precoated with a thin platinum film). The cross-section (inset) shows a 12- μm thick uniform porous film (height of the CNW), with the carbon sheets vertically oriented with respect to the surface of the substrate. It can also be noted that the open spaces between the carbon sheets extend across the layer from the top to the bottom. The porous

honeycomb structure consists of interconnected carbon sheets with lengths of 1-2 μm (top view SEM) and thicknesses of 10-50 nm. The graphene-type structure of the CNW is confirmed by Raman spectroscopy (Figure S1) and transmission electron microscopy (TEM) images (Figure S2). With electrodeposition, the CNW were covered in-depth, up to 6-7 μm , with the pseudo-capacitive hydrated RuO_2 particles (Figure 1b and S3). The particles have sizes in the range of hundreds of nanometers and are agglomerated in a cauliflower morphology (Figure 1b, S3 and S4). The nature of the electrodeposited layer is demonstrated by electron diffraction (inset of Figure S2a) and XPS (Figure S5). The porous structure of CNW and its high flexibility offer not only paths for electrolyte penetration, but also space for the volume expansion of the hRuO_2 material without any damage of the connectivity between the grains and the CNW, as represented in the schematic in Figure 1c. An intimate contact between the hRuO_2 particles and the CNW is observed in the cross-section SEM micrograph hRuO_2/CNW layered structure (Figure 1b). The interface between the two material types, distinguishable by their different morphology, is not actually defined. This was confirmed by high resolution TEM investigations (Figure 1d and S2): the RuO_2 nanoparticles with sizes of 1-3 nm lie on the graphene sheets composing the CNW (the amorphous hRuO_2 nanoparticles display crystalline characteristic as a result of their transformation upon irradiation by the e-beam of the microscope). Moreover, the hRuO_2 particles are distributed evenly, indicating the existence of a large connective area between the carbon wall and the pseudo-capacitive material (Figure S2b).

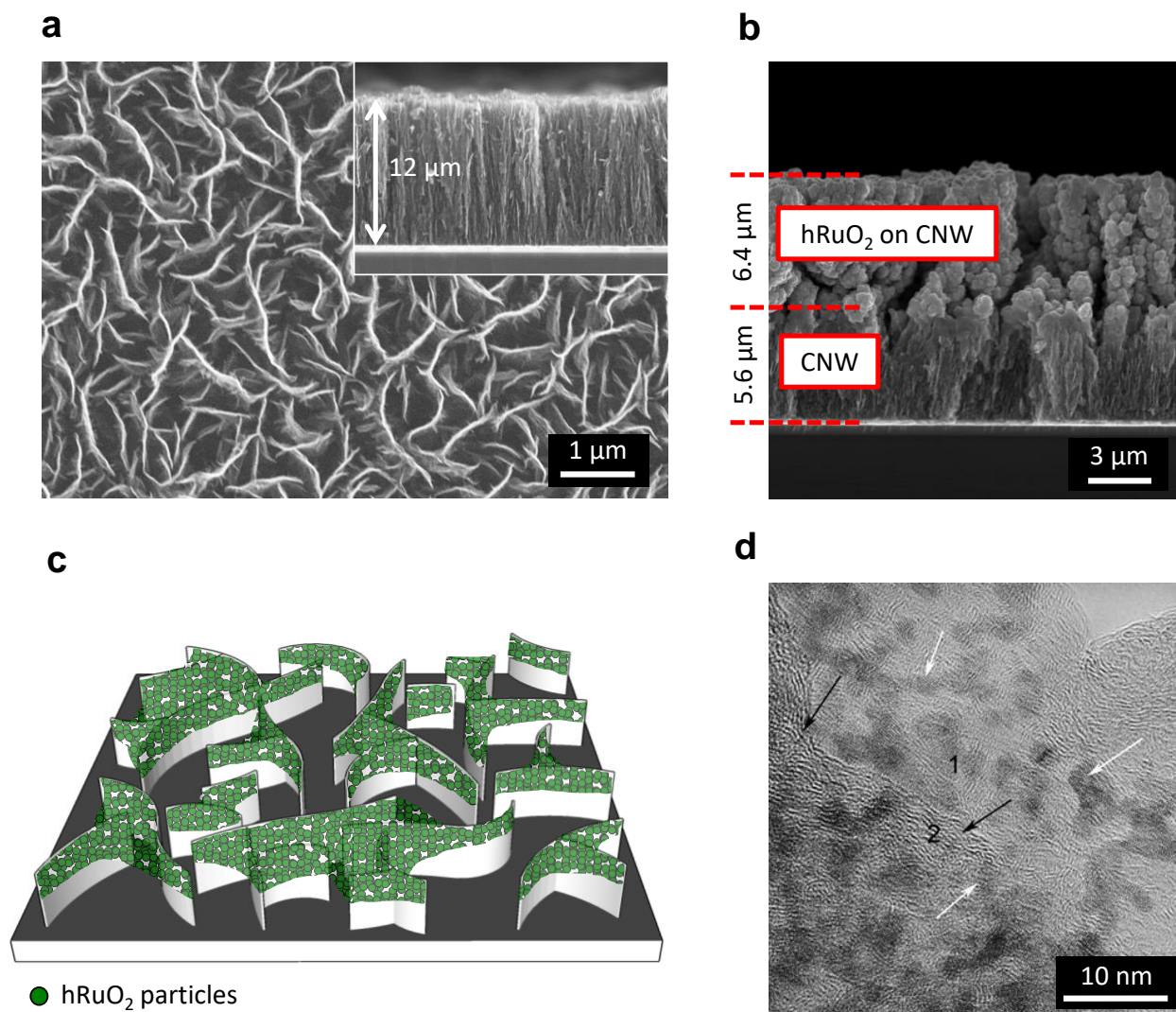


Figure 1 (a) Scanning electron microscope (SEM) image of a 12 μm-thick CNW film; inset: cross-section revealing the vertically aligned morphology of the CNW film. (b) Cross-section SEM image of a CNW film (bottom) on which hRuO₂ has been electrodeposited on its top. The two materials are distinguishable by their different morphology (cauliflower vs. vertically aligned). (c) Schematic of the vertically-aligned CNW decorated with hRuO₂ particles. (d) High resolution transmission electron microscopy (HRTEM) image showing the RuO₂ nanoparticles (some marked with white arrows), lying on the lateral faces (marked 1) and edges (marked 2) of

the CNW; black arrows indicate the lattice fringes of the (002) crystallographic planes visible at the CNW-edges (for more information see Figure S2).

The electrochemical performances of the CNW with thicknesses ranging from 900 nm to 12 μm were evaluated using cyclic voltammograms (CV). The specific capacitance of the CNW films increases with increasing thickness, up to 5.7 mF cm^{-2} for the 12 μm -thick CNW (Figure S6). This value is very close to the value of 18.3 mF cm^{-2} obtained by A. Achour *et al.* with titanium nitride/carbon nanotubes electrodes, which is the highest specific capacitance reported for electrodes in micro-supercapacitors [31,32].

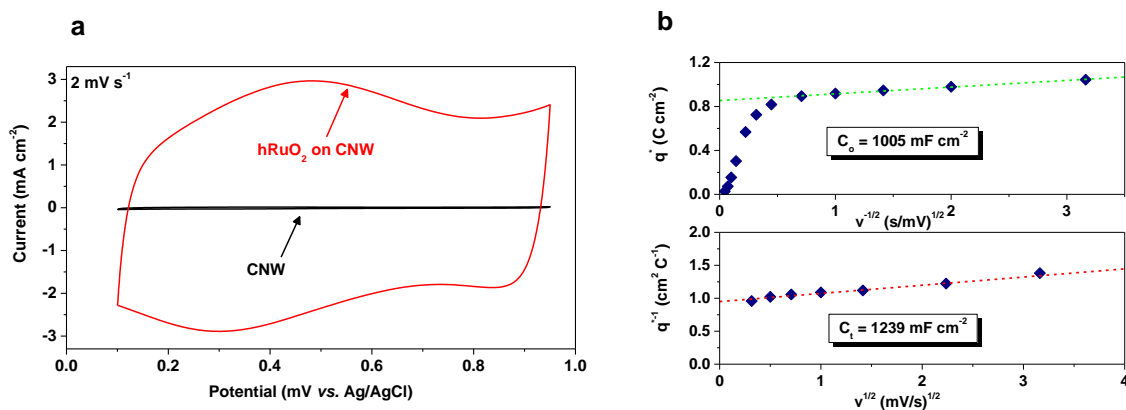


Figure 2 Electrochemical characterization of a CNW/hRuO₂ electrode. (a) CV of the 12 μm -thick CNW before and after hRuO₂ electrodeposition in de-aerated 0.5 M sulfuric acid electrolyte. (b) Variation of the voltammetric charge (q^*) with respect to the sweep rates.

Furthermore, high surface area hRuO₂ was afterwards synthesized using a 12 μm -thick CNW as a template (Figure S7). To our surprise, this hRuO₂/CNW hybrid electrode exhibited an extremely high capacitance of 1094 mF cm^{-2} when cycled at 2 mV s^{-1} in sulfuric acid electrolyte (Figure 2a), which is to our knowledge, an unprecedented performance for a microfabricated

supercapacitor electrode. The value of the outer capacitance (C_o), which is related to the more accessible active surface, reaches 1005 mF cm^{-2} for a total capacitance (C_t) of 1239 mF cm^{-2} (Figure 2b) [29]. This value is three orders of magnitude higher than that of the state-of-the-art graphene based micro-supercapacitors (0.3 mF cm^{-2} electrode capacitance) [11], and far larger than most micro-supercapacitor electrodes based on other advanced materials (Figure 3) [33-37].

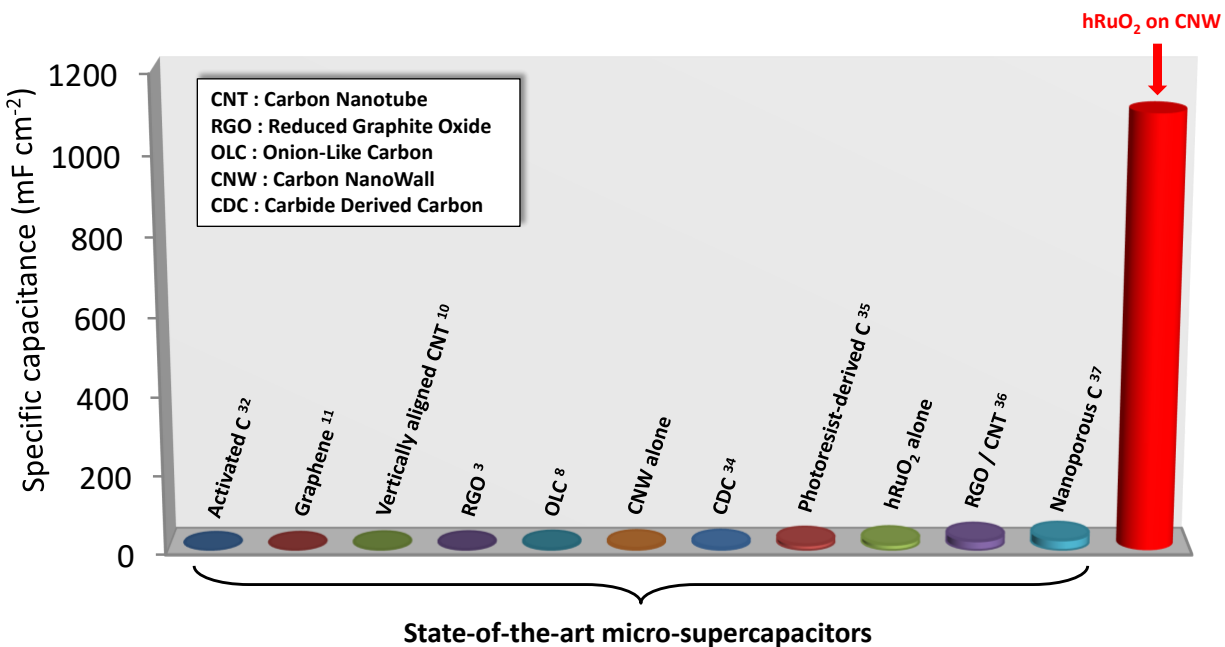


Figure 3 Comparison of the hybrid CNW/hRuO₂ electrode capacitance with the electrode capacitance of state-of-the-art micro-supercapacitors. (A factor of 4 has been taken into account between the electrode and the cell capacitance).

Figure S3 shows, for comparison, the morphology of a hRuO₂ thin film deposited on a flat gold substrate using the same experimental conditions. Its thickness is identical to the one deposited on CNW. The deposition kinetics does not seem modified by a change of the substrate, with a hRuO₂ able to grow on a large surface area. The C_o/C_t ratio of the CNW/hRuO₂ electrode (81 %) is also very close (and even higher) than the one obtained with hRuO₂ deposited on flat

gold substrate (71 %, Figure S8), indicating that, irrespective of the substrate differences for these two electrodes, most of the total storable charge is rapidly accessible.

Figure S9 shows the Nyquist plots in sulfuric acid electrolyte for the CNW before and after hRuO₂ electrodeposition. For both samples, no leakage current is observed, with a near vertical straight line in the low-frequency region typical of a capacitive behaviour. A negligible equivalent distributed resistance (EDR) and an equivalent series resistance (ESR) of 11.8 Ω cm² were estimated from the high frequency part of the spectrum of the hRuO₂-free CNW. The ESR slightly decreased to 8 Ω cm² when decorated with conductive hRuO₂, leading to a maximum specific power of 31.3 mW cm⁻².

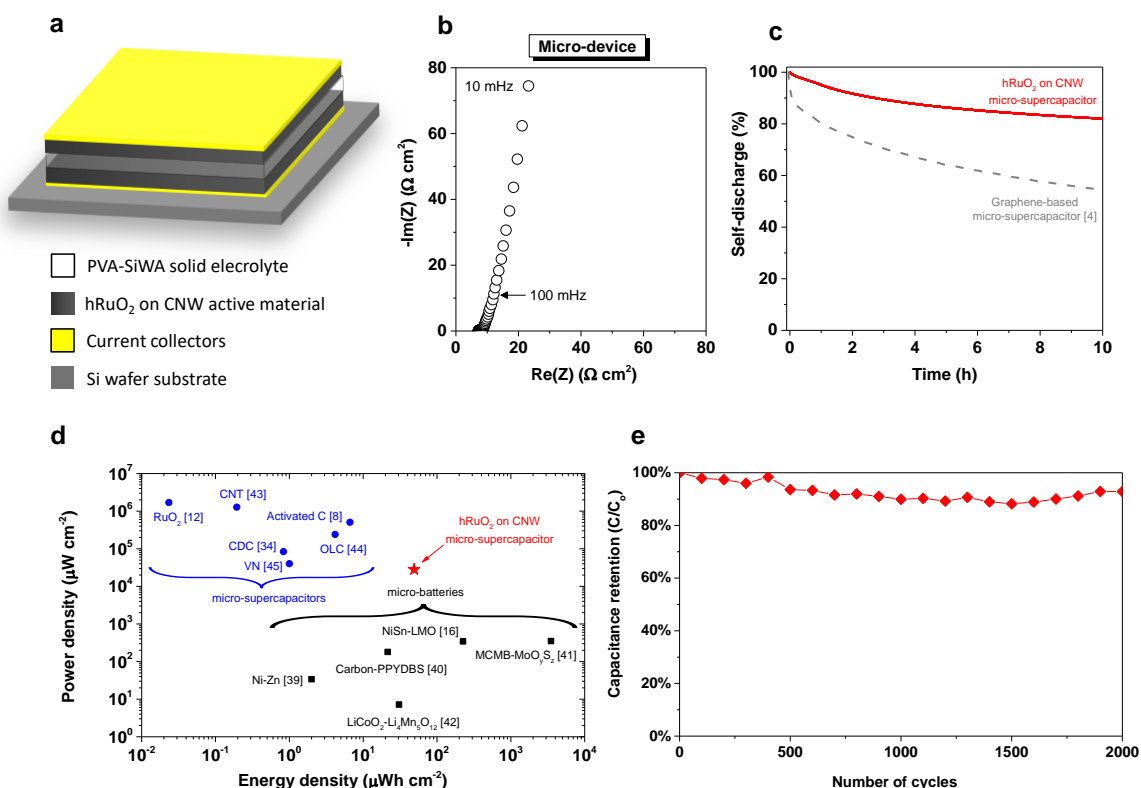


Figure 4 Characterization of a solid-state micro-supercapacitor based on CNW/hRuO₂. (a) Schematic diagram of on-chip micro-supercapacitor with 2D architecture. (b) Nyquist plot and

(c) self-discharge curve of the micro-device. (d) Comparison, in a Ragone plot, of the specific energy and power density of the CNW/hRuO₂-based micro-supercapacitor with state-of-the-art micro-supercapacitors and micro-batteries. (e) Evolution of the relative capacitance vs. the number charge/discharge cycles at 1.5 mA cm⁻².

Vertically-aligned CNW/hRuO₂ electrode has been employed to realize an-all-solid-state micro-supercapacitor in a stack configuration using a silicon wafer as a substrate (Figure 4a). An innovative solid-polymer electrolyte [38], composed of polyvinyl alcohol (PVA), orthophosphoric acid (H₃PO₄) and silicotungstic acid (SiWA) was used to act as a separator and ionic conductor without leakage issues and very low ESR (Figure 4b). The micro-device exhibits also a very low self-discharge (less than 18 % voltage drop after 10 h, Figure 4c), lower than that of a graphene-based micro-supercapacitor, which is known for good energy retention [4].

To demonstrate the overall performance of the solid-state micro-supercapacitor, a Ragone plot is shown Figure 4d [39-45]. Remarkably, this solid-state CNW/hRuO₂ micro-supercapacitor delivered a specific energy density of 49 μWh cm⁻² (*i.e.* 2 μWh cm⁻² μm⁻¹), which is higher than recent work reported for micro-supercapacitors [8, 12, 34, 43-45] and comparable to the state-of-the-art lithium ion micro-batteries [16, 39-42], but with much higher power and much higher lifetime (up to 2000 cycles of galvanostatic charge/discharge at 1.5 mA cm⁻², Figure 4e and Figure 5).

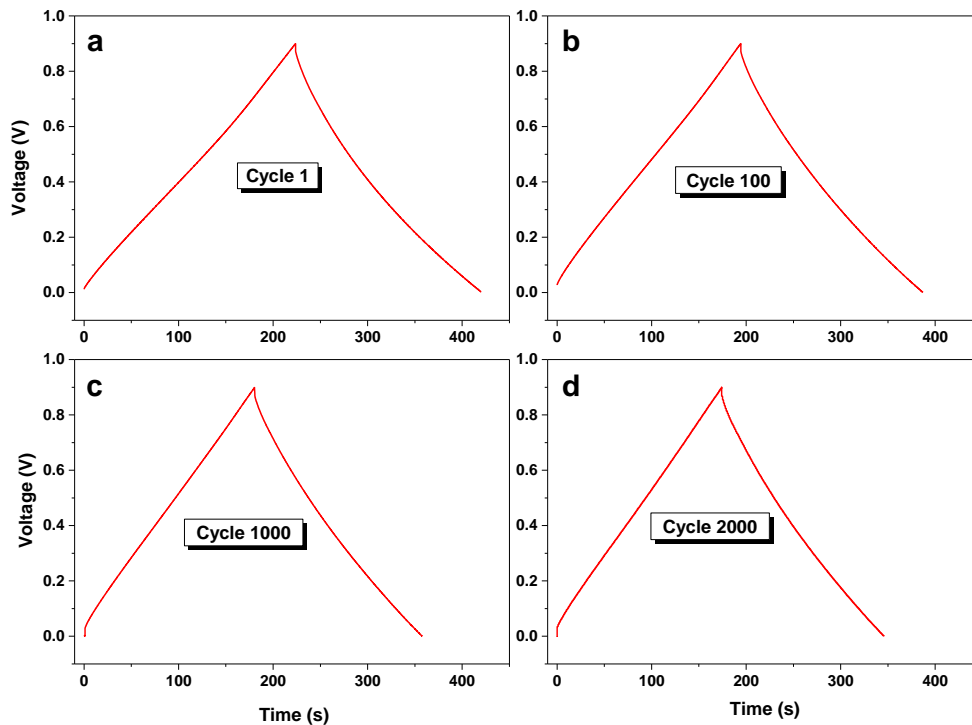


Figure 5 Galvanostatic charge/discharge curves at 1.5 mA cm^{-2} at different cycles of a solid-state CNW/hRuO₂-PVA/SiWa-CNW/hRuO₂ micro-supercapacitor. (a) 1st cycle. (b) 100th cycle. (c) 1000th cycle. (d) 2000th cycle.

Conclusions

The use of vertically-aligned CNW decorated with hRuO₂ particles offers an exceptional potential for micro-supercapacitors by patterning such electrode onto silicon wafers with standard microelectronic processes. For the first time, it is showcased that micro-supercapacitors can compete, in term of specific energy, with micro-batteries to power microelectronic devices such as wireless sensor nodes, active radiofrequency identification (RFID) tags and embedded micro-sensors. These applications can be extended to larger devices by scaling up the electrode

surface. Further improvements and optimization of the electrodeposition process for the hRuO₂ should also allow a substantial increase of the capacitance and energy of the device.

Acknowledgments

This work was financially supported by the French National Research Agency (ANR) through the MIDISTOCK project and the Ministry of National Education of Romania (CNCS – UEFISCDI, project numbers PN-II-ID-PCE-2012-4-0629 and PN-II-ID-PCE-2012-4-0362). One of us (D.G.) would like to acknowledge the financial support of the Canada Research Chair program.

Appendix. Supplementary materials

Supplementary data associated with this article can be found in the online version.

References

- [1] Z.L. Wang, *Adv. Mater.* 24 (2012) 280-285.
- [2] J. Chmiola, C. Largeot, P.L. Taberna, P. Simon, Y. Gogotsi, *Science* 328 (2010) 480-483.
- [3] W. Gao, N. Singh, L. Song, Z. Liu, A.L. Mohana Reddy, L. Ci, R. Vajtai, Q. Zhang, B. Wei, P.M. Ajayan, *Nat. Nanotech.* 6 (2011) 496-500.
- [4] M.F. El-Kady, R.B. Kaner, *Nat. Comm.* 4 (2012) 1475.
- [5] Q. Meng, H. Wu, Y. Meng, K. Xie, Z. Wei, Z. Guo, *Adv. Mater.* 26 (2014) 4100-4106.
- [6] I. Nam, G.P. Kim, S. Park, J.W. Han, J. Yi, *Energy Environ. Sci.* 7 (2014) 1095-1102.
- [7] S.K. Kim, H.J. Koo, A. Lee, P.V. Braun, *Adv. Mater.* 26 (2014) 5108-5112.
- [8] D. Pech, M. Brunet, H. Durou, P. Huang, V. Mochalin, Y. Gogotsi, P.L. Taberna, P. Simon, *Nat. Nanotech.* 5 (2010) 651-654.

- [9] K. Sheng, Y. Sun, C. Li, W. Yuan, G. Shi, *Sci. Rep.* 2 (2012) 247.
- [10] A. Ghosh, V.T. Le, J.J. Bae, Y.H. Lee, *Sci. Rep.* 3 (2013) 2939.
- [11] Z.-S. Wu, K. Parvez, X. Feng, K. Müllen, *Nat. Comm.* 4 (2013) 2487.
- [12] D. Pech, M. Brunet, T.M. Dinh, K. Armstrong, J. Gaudet, D. Guay, *J. Power Sources* 230 (2013) 230-235.
- [13] T.M. Dinh, K. Armstrong, D. Guay, D. Pech, *J. Mater. Chem. A* 2 (2014) 7170-7174.
- [14] Z.S. Wu, K. Parvez, X. Feng, K. Müllen, *J. Mater. Chem. A* 2 (2014) 8288-8293.
- [15] H. Zhang, X. Yu, P.V. Braun, *Nat. Nanotech.* 6 (2011) 277-281.
- [16] J.H. Pikul, H.G. Zhang, J. Cho, P.V. Braun, W.P. King, *Nat. Comm.* 4 (2013) 1732.
- [17] N.A. Kyeremateng, *ChemElectroChem* 1 (2014) 1442-1467.
- [18] W. Deng, X. Ji, Q. Chen, C.E. Banks, *RSC Adv.* 1 (2011) 1171-1178.
- [19] P. Simon, Y. Gogotsi, *Nat. Mater.* 7 (2008) 845-854.
- [20] Z.S. Wu, G. Zhou, L.C. Yin, W. Ren, F. Li, H.M. Cheng, *Nano Energy* 1 (2012) 107-131.
- [21] W. Wang, S. Guo, I. Lee, K. Ahmed, J. Zhong, Z. Favors, F. Zaera, M. Ozkan, C.S. Ozkan, *Sci. Rep.* 4 (2014) 4452.
- [22] X. Lang, A. Hirata, T. Fujita, M. Chen, *Nat. Nanotech.* 6 (2011) 232-236.
- [23] T.C. Hung, C.F. Chen, W.T. Whang, *Electrochem. Solid-State Lett.* 12 (2009) K41-K44.
- [24] D.H. Seo, S. Kumar, K. Ostrikov, *Carbon* 49 (2011) 4331-4339.
- [25] S. Vizireanu, G. Dinescu, L.C. Nistor, M. Baibarac, G. Ruxanda, M. Stancu, D. Ciuparu, *Physica E* 47 (2013) 59-65.
- [26] Z. González, S. Vizireanu, G. Dinescu, C. Blanco, R. Santamaría, *Nano Energy* 1 (2012) 833-839.
- [27] S. Hassan, M. Suzuki, S. Mori, A.A. El-Moneim, *J. Power Sources* 249 (2014) 21-27.

- [28] S. Vizireanu, S.D. Stoica, C. Luculescu, L.C. Nistor, B. Mitu, G. Dinescu, *Plasma Sources Sci. Technol.* 19 (2010) 034016.
- [29] S. Ardizzone, G. Fregonara, S. Trasatti, *Electrochim. Acta* 35 (1990) 263-267.
- [30] D. Baronetto, N. Krstajić, S. Trasatti, *Electrochim. Acta* 39 (1994) 2359-2362.
- [31] A. Achour, J.B. Ducros, R.L. Porto, M. Boujtita, E. Gautron, L. Le Brizoual, M.A. Djouadi, T. Brousse, *Nano Energy* 7 (2014) 104-113.
- [32] M. Beidaghi, Y. Gogotsi, *Energy Environ. Sci.* 7 (2014) 867-884.
- [33] L. Wei, N. Nitta, G. Yushin, *ACS Nano* 7 (2013) 6498-6506.
- [34] P. Huang, M. Heon, D. Pech, M. Brunet, P.L. Taberna, Y. Gogotsi, S. Lofland, J.D. Hettinger, P. Simon, *J. Power Sources* 225 (2013) 240-244.
- [35] B. Hsia, M.S. Kim, M. Vincent, C. Carraro, R. Maboudian, *Carbon* 57 (2013) 395-400.
- [36] M. Beidaghi, C. Wang, *Adv. Funct. Mater.* 22 (2012) 4501-4510.
- [37] C. Shen, X. Wang, W. Zhang, F. Kang, *Sci. Rep.* 3 (2013) 2294.
- [38] H. Gao, K. Lian, *J. Mater. Chem.* 22 (2012) 21272-21278.
- [39] F. Chamran, Y. Yeh, H.S. Min, B. Dunn, C. Kim, *J. Microelectromechanical Syst.* 16 (2007) 844-852.
- [40] H.S. Min, B.Y. Park, L. Taherabadi, C. Wang, Y. Yeh, R. Zaouk, M.J. Madou, B. Dunn, *J. Power Sources* 178 (2008) 795-800.
- [41] M. Nathan, D. Golodnitsky, V. Yufit, E. Strauss, T. Ripenbein, I. Shechtman, S. Menkin, E. Peled, *J. Microelectromechanical Syst.* 14 (2005) 879-885.
- [42] M. Kotobuki, Y. Suzuki, H. Munakata, K. Kanamura, Y. Sato, K. Yamamoto, T. Yoshida, *Electrochim. Acta* 56 (2011) 1023-1029.
- [43] T.M. Dinh, D. Pech, M. Brunet, A. Achour, *J. Phys. Conf. Ser.* 476 (2013) 012106.

[44] P. Huang, D. Pech, R. Lin, J.K. McDonough, M. Brunet, P.L. Taberna, Y. Gogotsi, P. Simon, *Electrochem. Comm.* 36 (2013) 53-56.

[45] E. Eustache, R. Frappier, R.L. Porto, S. Bouhtiyya, J.F. Pierson, T. Brousse, *Electrochem. Comm.* 28 (2013) 104-106.